Makara Journal of Technology

Volume 28 | Issue 2 Article 3

8-30-2024

Effect of Tibial Malrotation on Anterior and Posterior Cruciate Ligaments in Bicruciate-Retaining Total Knee Arthroplasty

Muhammad Saakeereen Sa'audi
School of Mechanical Engineering, College of Engineering, Universiti Teknologi MARA, Shah Alam 40450, Malaysia

Abdul Halim Abdullah
School of Mechanical Engineering, College of Engineering, Universiti Teknologi MARA, Shah Alam 40450, Malaysia

Solehuddin Shuib
School of Mechanical Engineering, College of Engineering, Universiti Teknologi MARA, Shah Alam 40450, Malaysia

Muhammad Azim Mat Raffei
School of Mechanical Engineering, College of Engineering, Universiti Teknologi MARA, Shah Alam 40450, Malaysia

Mohd Fairudz Mohd Miswan
Department of Orthopaedics and Traumatology, Faculty of Medicine, Universiti Teknologi MARA, Sungai Buloh 47000, Malaysia

See next page for additional authors

Recommended Citation

Sa'audi, Muhammad Saakeereen; Abdullah, Abdul Halim; Shuib, Solehuddin; Mat Raffei, Muhammad Azim; Mohd Miswan, Mohd Fairudz; and Mohd Anuar, Mohd Afzan (2024) "Effect of Tibial Malrotation on Anterior and Posterior Cruciate Ligaments in Bicruciate-Retaining Total Knee Arthroplasty," *Makara Journal of Technology*: Vol. 28: Iss. 2, Article 3.
DOI: 10.7454/mst.v28i2.1647
Available at: https://scholarhub.ui.ac.id/mjt/vol28/iss2/3

Effect of Tibial Malrotation on Anterior and Posterior Cruciate Ligaments in Bicruciate-Retaining Total Knee Arthroplasty

Cover Page Footnote

We would like to express our sincere gratitude to the College of Engineering, Universiti Teknologi MARA. This research was funded by Universiti Teknologi MARA, grant number 600-RMC/GPK 5/3 (098/2020).

Authors

Muhammad Saakeereen Sa'audi, Abdul Halim Abdullah, Solehuddin Shuib, Muhammad Azim Mat Raffei, Mohd Fairudz Mohd Miswan, and Mohd Afzan Mohd Anuar

Makara J. Technol. 28/2 (2024), 53–61
doi: 10.7454/mst.v28i2.1647

Effect of Tibial Malrotation on Anterior and Posterior Cruciate Ligaments in Bicruciate-Retaining Total Knee Arthroplasty

Muhammad Saakeereen Sa'audi[1], Abdul Halim Abdullah[1], Solehuddin Shuib[1], Muhammad Azim Mat Raffei[1], Mohd Fairudz Mohd Miswan[2], and Mohd Afzan Mohd Anuar[1*]

1. School of Mechanical Engineering, College of Engineering, Universiti Teknologi MARA, Shah Alam 40450, Malaysia
2. Department of Orthopaedics and Traumatology, Faculty of Medicine, Universiti Teknologi MARA, Sungai Buloh 47000, Malaysia

[*]*E-mail: afzan341@uitm.edu.my*

Abstract

Osteoarthritis (OA) is a musculoskeletal disorder specified as a joint disease that affects mostly human joints worldwide. Total knee arthroplasty (TKA) is performed to restore the affected joint and relieve the symptoms. However, tibial malrotation, which is one of the most common errors in TKA, results in poor function of the implant and pain after the procedure. People with OA often experience limited mobility and cannot accomplish daily tasks. Finite element analysis (FEA) has been widely applied to interpret the biomechanical and kinematic force along the joint and investigate the cruciate ligament's mechanical behavior. Unfortunately, one of the problems in TKA implants is their malalignment affecting tibial rotation. This study employs FEA to investigate the relationship between tibial malrotation and the consequent displacements and forces in the anterior cruciate ligament (ACL) and posterior cruciate ligament (PCL). A subject-specific knee model is used to study the effects of ligament model complexity and simulated ligament wrapping on knee biomechanics and kinematics. Tibial malrotation had a more considerable effect on ACL than on PCL. In terms of ligament forces, both anterior and posterior PCL bundles generated notably greater forces compared with the ACL bundles, with averages of 26823.92 ± 13.32 N and 2796.49 ± 23.98 N, respectively. The displacement of the PCL bundles was also substantial, equaling 26.37 ± 0.01 mm in the anterior and 18.87 ± 0.08 mm in the posterior. Correct implant alignment is essential to avoid overtensioning of the ligament and offers knee joint ligament balance that can restore native knee kinematics.

Keywords: bicruciate retaining, finite element analysis, ligament forces, malrotation, total knee arthroplasty

1. Introduction

In 2015, the World Health Organization estimated that 9.6% of men and 18.0% of women aged 60 years or older exhibited osteoarthritis (OA) symptoms, and that for those with symptomatic OA, 25% experienced difficulties in performing daily tasks and 80% suffered mobility restrictions [1, 2]. OA, which is a prevalent musculoskeletal disorder, results in joint pain, functional limitations, and reduced quality of life. OA primarily affects the hands, facet joints, feet, knees, and hips, with the knee being the most affected [3–5]. The knee is a weight-bearing joint, and its stiffness and dysfunction result in weakened muscles and limited flexion [4]. In OA, the damaged cartilage cannot be restored to its initial condition, hence necessitating total knee arthroplasty (TKA) surgery to treat it. However, the existing TKA designs cannot completely restore normal knee kinematics [6]. Although TKA effectively relieves pain and restores function, range of motion is a crucial factor influencing postoperative outcomes and is considerably affected by preoperative range of motion [7]. Compared with the conditions before OA, abnormal knee kinematics may persist even after TKA [8, 9].

Biomechanical testing methods, including *in vivo* and computational simulations, have been employed to assess TKA. They aim to evaluate the compatibility of TKA implant designs with natural human kinematics and kinetics, particularly focusing on the kinematic joint effects on cruciate ligament forces and concentration on tibial malrotation across various knee conditions. Malalignment during TKA surgery can result in tibial malrotation, often caused by measurement errors [7]. Although implant alignment should ideally replicate forces in a healthy knee, achieving this outcome is not

always feasible. Exceeding acceptable ranges of implant distortion can result in knee instability and affect kinematic joint behavior and cruciate ligament forces.

Computational approach is currently in demand, particularly finite element analysis (FEA), as acquiring live testing specimens is excessively challenging. Hence, a fully virtual environment has been used, employing three-dimensional (3D) models of TKA prostheses. This approach allows for examination of different virtual ligament complexities, component malalignments, and tibial malrotation. Strain and stress conditions within the tibia cannot be experimentally measured, hence justifying the reliance on computational analysis. A virtual TKA knee model with virtual ligaments can be used to assess the consequences of various factors. By developing and modifying a 3D finite element (FE) model of TKA implant design, we can investigate the effect of tibial rotation on stress distribution in the implant as well as quantify and establish correlations between tibial rotation, knee joint kinematics, and cruciate ligament forces.

TKA studies often focus on knee kinematics, particularly the impact on the cruciate ligament. Bicruciate-retaining total knee arthroplasty (BCR-TKA) designs aim to restore natural knee movement by preserving both the anterior cruciate ligament (ACL) and posterior cruciate ligament (PCL) [4, 10]. Previous research works have suggested that knees treated with BCR-TKA exhibit kinematics and stability comparable with those of healthy knees. However, several arguments have been raised regarding the clinical outcomes of BCR-TKA versus ACL-sacrificing TKA [4]. External and internal tibial rotations considerably influence the postoperative flexion angle of the knee [11]. In vivo, studies examining ligament forces during BCR-TKA have reported substantial alterations in knee kinematics during activities that involve deep knee bending, with these kinematic changes exhibiting a strong correlation with alterations in cruciate ligament forces [4, 12].

FEA is a flexible approach for conducting parametric comparative studies, allowing for manipulation of various design parameters and prediction of mechanical behaviors [13]. Simplified FE models incorporating basic geometry, cartilage, menisci, and ligament-driven kinetics have been observed to yield cartilage responses largely comparable to those of more complex models incorporating additional joint tissue features [12]. The recent investigations have also employed FE models to predict the gradual loss of proteoglycans and collagen in articular cartilage. Application of these models, particularly for the knee, can enhance our understanding of the biomechanical modifications associated with development of TKA [12, 13].

Therefore, this study constructs a 3D FE model of a BCR-TKA implant to investigate the effect of tibial malrotation on the mechanics of both the ACL and PCL. A patient-specific multibody dynamics model of TKA is developed. The knee model is constructed, starting with modeling of a BCR-TKA implant, and ligaments surrounding the knee are incorporated using spring elements. Tibial malrotation is simulated by altering the rotational position of the tibial component while retaining the same femoral alignment. Displacements and reaction forces in the ACL and PCL during knee bending motion are observed.

2. Methods and Analysis

3D models of the femoral component, tibial inserts, and tibial component were constructed on the basis of the geometrical landmark of a 29-year-old female (W = 70 kg, H = 170 cm) [14, 15]. Two deformable contact models were defined between the femoral component and tibial compartment. Ligaments, namely the medial collateral ligament (MCL), lateral collateral ligament (LCL), ACL, and PCL, were wrapped around the knee joint model. They were modeled as spring elements with a piecewise force–displacement relationship. Table 1 presents the stiffness coefficient assigned to each ligament [16]. Figure 1 shows a 3D model of the BCR-TKA implant, alongside the attached ligaments that connected the femur and tibia.

Tibial bone, patella, and femoral bone were excluded from the knee model, as we focused on stress distribution at the tibiofemoral articulations between the TKA components to optimize the computational efficiency. For boundary conditions, the tibia component was mechanically constrained in all degrees of freedom while the femoral component was modeled to undergo bending motion ranging from 0° to 90° of flexion angle. Axial load, anterior–posterior (AP) load, and knee joint moment were applied to the reference point of the femoral component. Figure 2 shows the loading boundary applied to the knee model obtained from Bergmann *et al*. [17].

Table 1. Stiffness Coefficient of the Ligaments [16]

Ligament	Stiffness (N/mm)
ACL	380
LCL	100
MCL	100
PCL	200

Abbreviations: ACL = anterior cruciate ligament; LCL = lateral collateral ligament; MCL = medial collateral ligament; PCL = posterior cruciate ligament

(a) (b)

Figure 1. Three-Dimensional (3D) Model of the Bicruciate-Retaining Total Knee Arthroplasty (BCR-TKA) Implant Aligned with the Anteromedial and Posterolateral Bundles of Both the Anterior Cruciate Ligament (ACL) and Posterior Cruciate Ligament (PCL), Medial Collateral Ligament (MCL), and Lateral Collateral Ligament (LCL): (a) Isometric View and (b) Front View

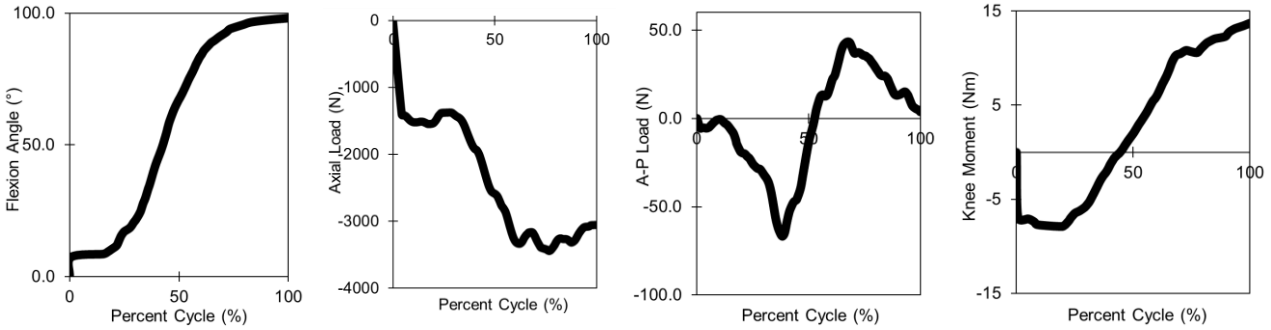

(a) (b) (c) (d)

Figure 2. Boundary and Loading Conditions: (a) Flexion Angle, (b) Axial Load, (c) Anterior–Posterior Load, and (d) Knee Joint Moment During Knee Flexion [17]

Figure 3. 3D FE Model of the BCR-TKA Implant

Table 2. Mechanical Properties of the Ultrahigh Molecular Weight Polyethylene (UHMWPE) used in this Study [21]

Material	Density (ton/mm^3)	Young's modulus (MPa)	Yield strength (MPa)	Poisson's ratio
UHMWPE	9.5×10^{-10}	1200	14.07	0.46

An FE mesh was generated using linear hexahedral solid (C3D8R) elements. High-gradient areas of the mesh were refined to ensure accurate representation of the model. The characteristic element length of 1.2 mm was employed in consistency with previous FE models [18–20]. Figure 3 shows the FE model of the BCR-TKA implant. Ultrahigh molecular weight polyethylene (UHMWPE, ISO5834-2) was used as the material for the tibial insert, and it was homogeneous, isotropic, and linearly elastic. Table 2 presents the mechanical properties of UHMWPE [21]. "Hard" pressure-overclosure relationship with a friction

coefficient of 0.04 was employed to simulate the contact between the femoral component and tibial insert [22, 23].

According to the patient's surgical report, the proximal tibia was cut at 90° to the long axis in the coronal plane (0° varus) and at 90° in the sagittal plane (0° posterior tilting). These positions were defined in the developed patient-specific multibody dynamics model of TKA as the neutral positions of the femoral and tibial components. The rotational positions of the tibial component were modified concerning the neutral position to investigate the tibial component's malrotation: neutral, and internal–external (IE) rotations of 3° and 10°. These tibial components with the same femoral component were separately imported into the developed patient-specific multibody dynamics model of TKA. We investigated the effects of the tibial component's malrotation on the ACL and PCL mechanics with the same tibiofemoral conformity. In mechanically aligned TKA, several reference lines were used to minimize IE malrotation of the femoral and tibial components [7].

This was accomplished in part by setting the AP axes of the femoral and tibial components as parallel to the flexion-extension plane of the extended knee. Several points and axes in the anteroposterior and mediolateral planes were described to aid in rotational alignment of the tibial component. The "Akagi line" is the most commonly used anatomical anteroposterior axis for tibial rotation. The degree of rotation that causes symptoms and initiates the need for further treatment considerably varies, ranging from 2° to 10° of internal rotation. Establishing a specific safe range for tibial rotation is difficult because several studies have reported positive results even in patients with degree of rotation outside the normal range. Mobile-bearing implants, however, are more forgiving of slight rotational errors [24].

3. Results and Discussion

ACL and PCL displacements. Displacement analysis of the anteromedial ACL bundle (aACL) and posterolateral ACL bundle (pACL) was conducted during knee flexion at various tibial rotation angles. At the neutral position (0°) of the tibial insert, the aACL exhibited a displacement of 4.234 mm as the knee flexed from 0° to 90°. An external tibial rotation of 3° resulted in a slightly lower displacement of 4.07 mm, while a further external rotation of 10° increased the displacement to 4.165 mm at the maximum flexion. Likewise, internal tibial rotations of 3° and 10° resulted in displacements of 3.990 and 3.574 mm, respectively, both of which were slightly lower than the displacement at the neutral position. During the early stage of knee flexion, all tibial rotation conditions exhibited steep increment in displacement, peaking at angles ranging from 40.5° to 45°. Subsequently, the aACL exhibited a regressive trend in displacement as the knee flexed to the maximum angle of 90°, with external rotations showing higher displacement compared with internal rotations. No considerable differences in kinematics were observed between the minimum and maximum flexion angles for both internal and external tibial rotations, except for the 10° internal tibial rotation condition, which showed slightly lower displacement compared with the other conditions.

The pACL exhibited the highest displacement of 4.40 mm during knee flexion at 3° external tibial rotation, compared with 4.244 displacement mm at the neutral position. As the tibia rotated further to 10° external tibial rotation, the pACL exhibited a displacement of 4.319 mm and no considerable differences were observed between each external rotation. The pACL exhibited 4.51 and 4.967 mm displacements at internal tibial rotations of 3° and 10°, respectively. Internal tibial rotation resulted in higher movement of the ligament versus external rotation, although no notable differences were observed compared with the neutral position. Both the aACL and pACL exhibited gradual increase in displacement, with similar values, during the early stages of knee flexion, i.e., from 0° to 13.5°. However, with the knee reaching the mid-flexion range, the displacement of the pACL gradually regressed until 49.5° flexion. Meanwhile, the displacement of the aACL continued to gradually regress until the maximum flexion angle. Interestingly, the pACL exhibited steep increases in displacement for knee flexion ranging from 49.5° to 90° across all tibial rotation conditions. Excessive tightness during knee flexion can impede the kinematic movement of the tibial component [25]. Figure 4 shows the ligament displacements at various flexion angles for both the aACL and pACL.

Displacement of the anterolateral bundle of the PCL (aPCL) remained consistent and exhibited similar patterns for each degree of tibial rotation during knee flexion, from the minimum to maximum value of the range. Figure 5 shows the ligament displacements at various flexion angles for both aPCL and posteromedial bundle of the PCL (pPCL). Clearly, the differences in displacement for each degree of tibial rotation are not considerable. Notably, the displacement of the aPCL sharply increased as the knee flexed between 31.5° and 54°. Similarly, the pPCL followed a comparable trend during knee flexion, exhibiting a similar distribution of displacement across all tibial rotation conditions. However, despite experiencing the same steep increment during the corresponding phase, the pPCL exhibited slightly lower displacement than the aPCL. In the initial phase, both the aPCL and pPCL exhibited moderate increase in displacement as the knee flexed from the starting position to the one-third point of flexion. This was followed by steep rise in displacement during the middle phase of knee flexion, and finally, a moderate increment toward the final quarter of flexion until reaching the maximum flexion. The reported changes in

ligament length were based on kinematic measurements, as experimental measurements of ligament length often involve measurement of the length between ligament insertions during replicated knee motion. A previously conducted study reported considerable overstretching of the PCL for deep flexion positions in BCR-TKA [26]. Nature or type of high-flexion activity was also observed to affect knee kinematics [4]. Figure 5 shows ligament displacements for knee joint motions at various flexion angles.

ACL and PCL forces. The forces exerted by the aACL and pACL exhibited different patterns during knee flexion across various tibial malrotation conditions. Figure 7 shows the ligament forces at various flexion angles for both aACL and pACL. In the early phase of flexion, i.e., from 4.5° to 18°, the aACL consistently exerted forces of 70 N across all simulated conditions, including a neutral position, and IE tibial malrotations of 3° and 10°. The highest force recorded was 982.151 N, which occurred during 3° internal tibial malrotation at 54° knee flexion. During the middle phase of flexion, i.e., from 36° to 54°, the forces gradually and steadily increased to reach their peak. Toward the end of knee flexion, all tibial malrotation conditions exhibited almost identical forces, although 10° internal tibial malrotation resulted in slightly lower forces on the aACL. We observed slight variations in forces among the various tibial malrotation conditions. As the knee approached the maximum flexion from the middle phase, only 10° internal tibial malrotation exhibited a gradual decrease in forces, while the other conditions resulted in fluctuating forces over the flexion angle during the mid-to-end phase of knee flexion.

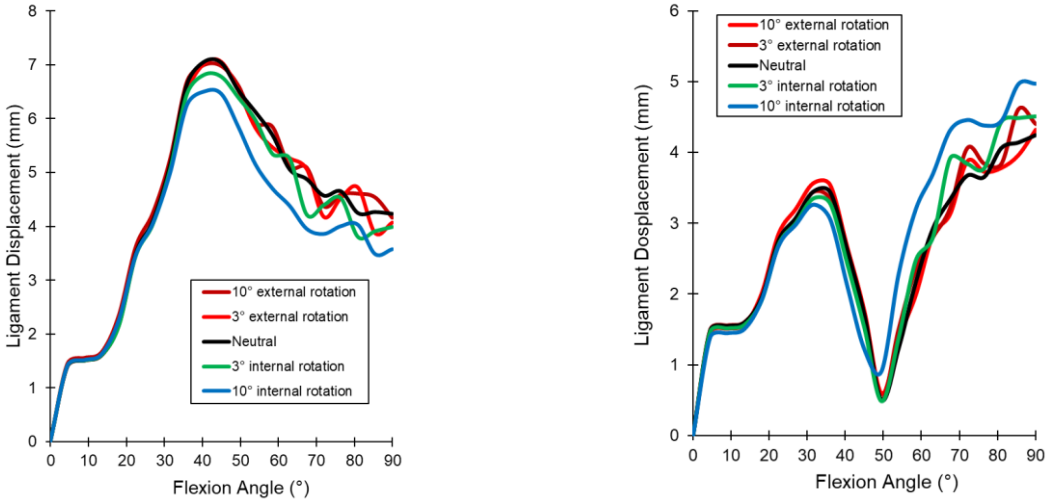

(a) (b)

Figure 4. Ligament Displacements at Various Flexion Angles for the (a) Anteromedial Bundle of the ACL (aACL) and (b) Posterolateral Bundle of the ACL (pACL)

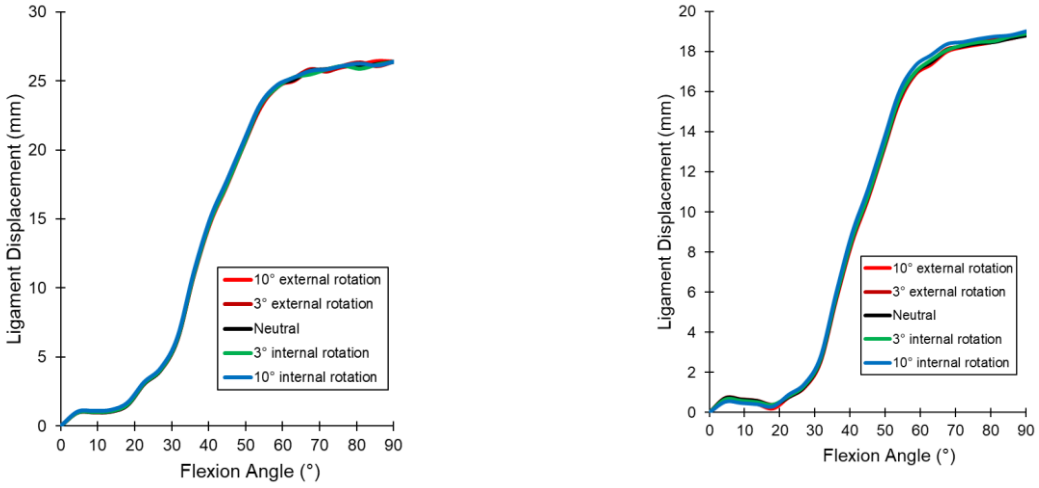

(a) (b)

Figure 5. Ligament Displacements at Various Flexion Angles for the (a) aPCL and (b) pPCL

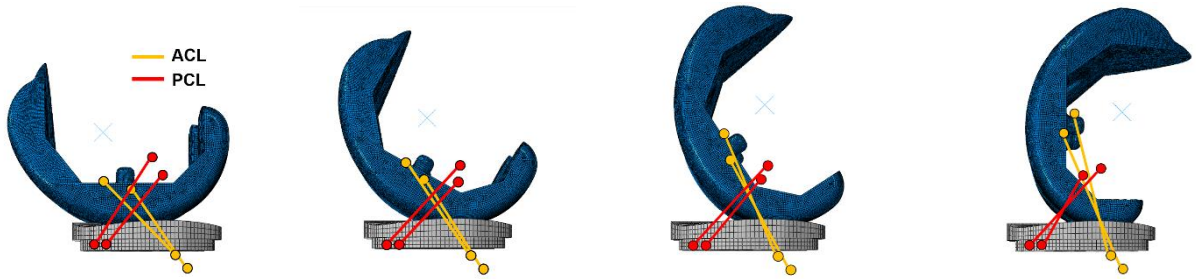

Figure 6. Displacements of the ACL and PCL at Flexion Angles of (a) 0°, (b) 30°, (c) 60°, and (d) 90°

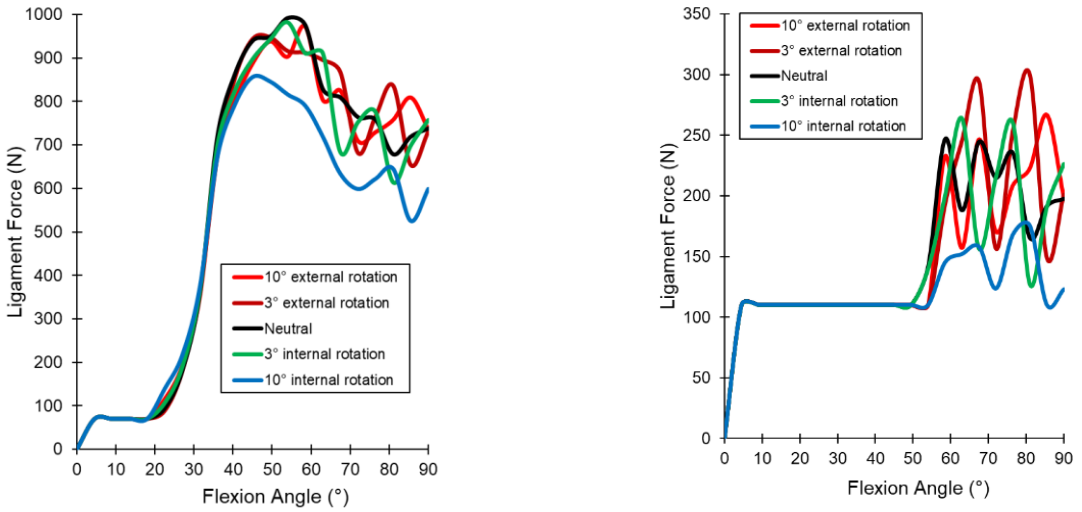

Figure 7. Ligament Forces at Various Flexion Angles for the (a) aACL and (b) pACL

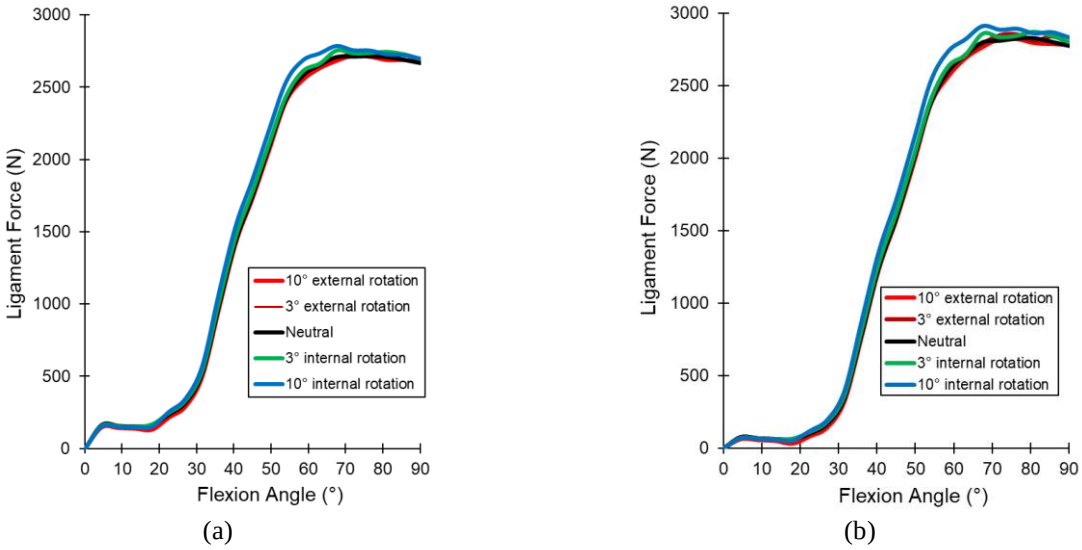

Figure 8. Ligament Forces at Various Flexion Angles for the (a) aPCL and (b) pPCL

The forces exerted on the pACL peaked during 3° external tibial malrotation at 81° knee flexion. External malrotation of the tibial component, which can occur during knee flexion, may become more apparent during knee extension [27]. However, these forces did not remain high as the knee continued to flex. Throughout the initial phase of flexion up to the mid-flexion point at 49.5°, forces equivalent to 110 N were generated across all tibial malrotation conditions, hence forming a plateau. The forces fluctuated as the knee flexed from the mid to

maximum range, exhibiting rapid changes for each tibial malrotation condition. This resulted in varying trends of declining and rising forces upon reaching the maximum flexion. During the final phase of flexion, we observed considerable differences in forces exerted on the pACL among various tibial malrotation conditions. The lowest force in this phase was observed to be 110 N during 10° internal tibial malrotation; the phase ended with slightly lower forces compared with those at the other conditions, at 122.8 N. Notably, tibial malrotation in the neutral position (0°) and 3° IE rotation resulted in almost identical forces when the knee reached the maximum flexion. Hence, we can infer that different types of high-flexion activities might distinctly affect ACL forces [4].

Figure 8 shows the ligament forces at various flexion angles for both the aPCL and pPCL. The aPCL and pPCL forces increased with flexion across all tibial malrotation conditions. At a flexion range of 31.5°–63°, the forces considerably increased and the force at 10° internal malrotation was higher than those at other conditions. We observed no considerable differences among the conditions as the knee flexed at the starting phase, ranging from 4.5° to 22.5° of flexion. Subsequently, as the knee reached the maximum flexion, the forces steadily decreased and the force in the aPCL did not considerably change at various malrotations of the tibial component. The aPCL exhibited no difference in variation of forces exerted during the IE malrotation.

Similar to that for the aPCL, forces in the pPCL increased with knee flexion for various IE tibial malrotation conditions. Forces exerted during the early stage of flexion, i.e., 4.5° to 22.5°, showed no considerable changes for each condition, and no notable differences in forces were identified between the tibial malrotation conditions. Through the middle phase of the flexion, i.e., from 31.5° to 67.5°, similar to that for the aPCL, forces in the pPCL steeply increased and peaked across all conditions; the highest force, 2911.63 N, was exerted during 10° internal malrotation. In fact, 10° internal malrotation remained to provide the highest force up until the maximum knee flexion. At the maximum flexion, we observed no considerable differences among the various tibial malrotation conditions. Functional outcomes were adversely affected by a rotational mismatch of 10°. A previously conducted study demonstrated that better clinical outcomes were achieved when mean tibial component rotational angles ranged from 3° external rotation to 3° internal rotation [27]. Furthermore, overstretching of the PCL can increase the force exerted on the ligament. [28].

Bicruciate-retaining (BCR) TKA, which aims to replicate native knee kinematics by preserving the ACL, has yielded promising results in terms of joint stability and clinical outcomes [29]. BCR-TKA has been observed to considerably alter knee kinematics during deep knee bending activities. These changes in kinematics have shown a significant correlation with modifications in cruciate ligament forces. We believe these findings are important for development of suitable ligament-balancing strategies and advancement of BCR knee designs [4]. However, some studies have raised concerns regarding the elevated tension on the ligaments in BCR-TKA, which may result in higher revision rate and adversely affect clinical outcomes [30]. Internal rotation of the tibial component exceeding 3° results in higher stress on the patella, tilting, and misalignment. An internal rotation error of more than 5° is associated with anterior knee pain. Internal rotation exceeding 10° can cause stiffness. Malrotation exceeding 15° increases wear on the implant, exerts more tension on the surrounding ligaments, and ultimately results in failure of the joint replacement. However, an external rotation of up to 5°–10° is generally better tolerated [24]. Although research and development in BCR-TKA is ongoing, only a limited number of studies have compared BCR-TKA with the traditional cruciate-substituting TKA. Accordingly, further research must be conducted to establish knee prostheses that can more effectively preserve native knee kinematics [25]. This ongoing research is expected to contribute to advancing the field of TKA and improving the outcomes for patients in future. The finding suggest that the posterior ligaments exhibit varying patterns of length change at different locations. The parameters used for the ligament models were based on values from the literature to demonstrate the general workflow. However, determining the zero-load lengths of ligaments is a challenging task, and these parameters can considerably affect computational models. The sensitivity study demonstrated the sensitivity of ligament length change to model parameters. The model successfully captured the trend of ligament behavior vis-à-vis implant alignment [28].

We acknowledge certain limitations of this study. First, the study focused on a single model, which may limit generalizability of the findings. Future research could, therefore, involve testing on multiple models with various knee geometries or kinematically aligned implants in a bid to strengthen the results, allowing for more robust statistical analysis and more definitive conclusions. Second, the limited number of samples for each tibial malrotation condition warrants a mention, as the absence of alternative models for BCR-TKA design prevented the inclusion of design variations in the simulations. However, running multiple simulations for each condition might yield similar outcomes, minimizing the need for extensive computational testing. Third, we must recognize that the evaluation of the relationship between tibial malrotation, and cruciate ligament force and kinematics was based on computational approaches rather than real-life experiments, which may limit generalizability of the findings. Further research using experimental approaches is, thus, needed to comprehensively understand cruciate ligament behavior in the context of tibial malrotation.

Furthermore, assessment of bone coverage of the tibial component is a crucial factor affecting the component's rotation angle and clinical outcomes. However, the precise measurement of the contact area between the tibial component and bone was not feasible in this study. Plus, the scope of this study was limited to conditions with normal knee OA, excluding those with valgus and varus deformities.

4. Conclusion

This study demonstrated that tibial malrotation considerably influenced the kinematics and forces of the cruciate ligaments. The findings highlight the importance of considering tibial malrotation in ligament-balancing strategies and BCR knee designs to optimize joint stability and functional outcomes. However, the study has certain limitations, including the focus on a single model rather than multiple models and the use of computational approaches rather than real-life experiments. Hence, further research involving multiple models, experimental approaches, and larger-scale studies encompassing various knee OA conditions is needed to confirm and expand these findings. By gaining a deeper understanding of the relationship between tibial malrotation and cruciate ligament behavior, future advancements in TKA can be made to

1. preserve native knee kinematics in a more effective manner, and
2. improve the clinical outcomes.

Acknowledgment

We would like to express our sincere gratitude to the College of Engineering, Universiti Teknologi MARA. This research was funded by Universiti Teknologi MARA, Grant number 600-RMC/GPK 5/3 (098/2020).

References

[1] J. Lim, J. Kim, S. Cheon, Int. J. Environ. Res. Pu. 16/7 (2019) 1281.
[2] M.H.F. Keulen, J. Most, M.G.M. Schotanus, E.H. van Haaren, I.C. Heyligers, B. Boonen, J. Clin. Orthop. Trauma. 29 (2022) 101873.
[3] I.G. Arslan, J. Damen, M. de Wilde, J.J. van den Driest, P.J.E. Bindels, J. van der Lei, D. Schiphof, S.M.A. Bierma-Zeinstra, Arthrit. Care Res. 74/6 (2022) 937.
[4] K.M. Leyland, L.S. Gates, M.T. Sanchez-Santos, M.C. Nevitt, D. Felson, G. Jones, J.M. Jordan, A. Judge, D. Prieto-Alhambra, N. Yoshimura, J.L. Newton, L.F. Callahan, C. Cooper, M.E. Batt, J. Lin, Q. Liu, R.J. Cleveland, G.S. Collins, N.K. Arden, PCCOA Steering Committee Aging Clin. Exp. Res. 33/3 (2021) 529.
[5] O.J. Morgan, R. Hillstrom, H.J. Hillstrom, S.J. Ellis, Y.M. Golightly, R. Russell, M.T. Hannan, J.T. DelandIII, R. Hillstrom, ACR Open Rheumat. 1/8 (2019) 493.
[6] K. Kono, H. Inui, T. Tomita, T. Yamazaki, S. Konda, S. Taketomi, S. Tanaka, D.D. D'Lima, Sci. Rep. vol. 11 (2021) 5645.
[7] Y. Mikashima, T. Tomatsu, M. Horikoshi, T. Nakatani, S. Saito, S. Momohara, S.A. Banks, Clin. Biomech. 25/1 (2010) 83.
[8] J.S. Luttjeboer, M.R. Bénard, K.C. Defoort, G.G. van Hellemondt, A.B. Wymenga, J. Arthroplasty. 31/12 (2016) 2672.
[9] A.J. Nedopil, S.M. Howell, M.L. Hull, Orthop. Clin. N. Am. 47/1 (2016) 41.
[10] L.A. Montgomery, MSE Thesis, Department of Biomedical Engineering, Faculty of Engineering Science, The University of Western Ontario, Canada, 2021.
[11] M. Hanada, K. Hotta, H. Furuhashi, H. Koyama, Y. Matsuyama, Knee. 27/5 (2020) 1467.
[12] P.O. Bolcos, M.E. Mononen, A. Mohammadi, M. Ebrahimi, M.S. Tanaka, M.A. Samaan, R.B. Souza, X. Li, J.-S. Suomalainen, J.S. Jurvelin, J. Töyräs, R.K. Korhonen, Sci. Rep. 8/1 (2018) 17351.
[13] A.Z.E.-A. Arab, A. Merdji, A. Benaissa, S. Roy, B.-A.B. Bouiadjra, K. Layadi, A. Ouddane, O.M. Mukdadi, Comput. Methods Programs Biomed. 192 (2020) 105446.
[14] T.M. Guess, S. Razu, Med. Eng. Phys. 41 (2017) 26.
[15] T.M. Guess, S.S. Razu, K. Kuroki, J.L. Cook, J. Knee Surg. 31/1 (2018) 68.
[16] P.O. Bolcos, M.E. Mononen, A. Mohammadi, M. Ebrahimi, M.S. Tanaka, M.A. Samaan, R.B. Souza, X. Li, J.-S. Suomalainen, J.S. Jurvelin, J. Töyräs, R.K. Korhonen, Sci. Rep. 8/1 (2018) 17351.
[17] G. Bergmann, A. Bender, F. Graichen, J. Dymke, A. Rohlmann, A. Trepczynski, M.O. Heller, I. Kutzner, PLoS One. 9/1 (2014) e86035.
[18] O.-R. Kwon, K.-T. Kang, J. Son, S.-K. Kwon, S.-B. Jo, D.-S. Suh, Y.-J. Choi, H.-J. Kim, Y.-G. Koh, J. Orthop. Res. 32/2 (2014) 338.
[19] M.A.M. Anuar, M. Todo, R. Nagamine, Int. J. Biosci. Biochem. Bioinformat. 4/6 (2014) 428.
[20] Y.G. Koh, K.M. Park, H.Y. Lee, K.T. Kang, Bone Joint Res. 8/3 (2019) 156.
[21] P. Moewis, S. Checa, I. Kutzner, H. Hommel, G.N. Duda, PLoS One. 13/2 (2018) e0192225.
[22] Y.-G. Koh, J.-H. Nam, K.-T. Kang, J. Exp. Orth. 5/1 (2018) 53.
[23] A.C. Godest, M. Beaugonin, E. Haug, M. Taylor, P.J. Gregson, J. Biomech. 35/2 (2002) 267.
[24] R.N. Tandoğan, P.F. Indelli, M. Saffarini, A.S. Panni, E. Erçin, Tibial Rotational Alignment in Total Knee Arthroplasty Preliminary Report of the Tibial Rotation Study Group of European Knee Associates (EKA), 2017.
[25] M. Fujita, T. Matsumoto, N. Nakano, K. Ishida, Y. Kuroda, T. Maeda, S. Hayashi, R. Kuroda, Knee. 38

(2022) 69.
[26] K. Kono, H. Inui, T. Tomita, D.D. D'Lima, T. Yamazaki, S. Konda, S. Taketomi, R. Yamagami, K. Kawaguchi, S. Sameshima, T. Kage, S. Tanaka, Sci. Rep. 11 (2021) 18233.
[27] M. Fujita, T. Hiranaka, B. Mai, T. Kamenaga, M. Tsubosaka, K. Takayama, R. Kuroda, T. Matsumoto, Knee. 30 (2021) 70.
[28] V. Vanheule, H.P. Delport, M.S. Andersen, L. Scheys, R. Wirix-Speetjens, I. Jonkers, J. Victor, J.V. Sloten. Med. Eng. Phys. 40 (2017) 56.
[29] C. Zhou, Y. Peng, S. An, H. Bedair, G. Li, Arch. Orthop. Trauma. Surg. 142/9 (2022) 2313.
[30] C.K. Boese, S. Ebohon, C. Ries, D. De Faoite, Arch. Orthop. Trauma. Surg. 141/2 (2021) 293.